*Inorg. Chem.* **2008**, *47*, 322–332

# Exchange Interactions and Electron Delocalization in the Mixed-Valence Cluster $V_4^{IV}V_2^{V}O_7(OC_2H_5)_{12}$

**Maria A. Augustyniak-Jabłokow,[†] Charles Daniel,[‡] Hans Hartl,[‡] Johann Spandl,[‡] and Yurii V. Yablokov*,[†]**

*Institute of Molecular Physics PAS, Smoluchowskiego 17, 60 179 Poznań, Poland, and Institute of Chemistry and Biochemistry/Inorganic Chemistry, Freie Universität Berlin, Fabeckstrasse 34-36, 14195 Berlin, Germany*

Received April 12, 2007

The mixed-valence cluster compound $V_4^{IV}V_2^{V}O_7(OC_2H_5)_{12}$ was studied by X-band electron paramagnetic resonance (EPR) in the temperature range of 4.2–293 K. According to X-ray diffraction study, the crystal structure of the compound was described by a $R\bar{3}m$ space group at 295 K (four $d^1$ electrons are equally delocalized on all vanadium ions) and changed to a $P2_1/n$ space group on cooling the crystals to 173 K (the electrons are preferably localized on the four equatorial vanadium ions). The EPR spectra originate from the $S = 1$ total spin states with the fine structure averaged to a single Lorentzian line and from the $S = 2$ total spin states with fine structure partly averaged in the temperature range of 295–200 K and well averaged below 45–50 K. The states of $S = 1$ and $S = 2$ of comparable energy ($\Delta E \sim 2$ cm$^{-1}$; $E_{S=1} < E_{S=2}$) were shown to be the lowest ones. The $V^{IV} \leftrightarrow V^{V}$ unpaired electron transfers together with isotropic Heisenberg exchange were shown to determine the total spin states composition and the intracluster dynamics of the compound. Two types of electron transfers were assumed: the single-jump transfer leading to the averaged configurations of the $V_4^{IV}V_2^{V} \leftrightarrow V_3^{IV}V^{V}$ $V^{IV}V^{V}$ type and to the splitting of the total spin states by intervals comparable in magnitude with the isotropic exchange parameter $J \sim 100$ cm$^{-1}$ and the double-jump transfer resulting in dynamics. Temperature dependence of the transition rates $\nu_{tr}$ was observed. In the range of 295–210 K, the value of $\nu_{tr} = (0.5–0.6) \times 10^{10}$ s$^{-1}$ is sufficient for averaging the fine structure of the $S = 1$ states, and below 45 K the value of $\nu_{tr} \approx 1.5 \times 10^{10}$ s$^{-1}$ also averages the fine structure of the $S = 2$ state. A change in the localization plane of the $V^{IV}$ ions in the temperature range of 40–50 K was discovered.

## Introduction

A characteristic feature of multinuclear mixed-valence clusters of 3d ions is the coexistence of the exchange interaction and electron-transfer phenomena.[1−7] Both these phenomena affect spin energy levels of individual ions: The exchange interaction transforms them into a set of total spin states with intervals being multiple of the interaction parameter $J$, while the electron transfers lead to the additional splitting and shift of the spin states, which can be described by some parameters. The composition of available spin states is determined by the topology of the cluster and the conditions of delocalization of unpaired electrons.[8−13] The exchange clusters, including mixed-valence ones, containing from 5 to 10 and more 3d ions, can be considered as units intermediate between a complex and a molecular magnet,

* To whom correspondence should be addressed. E-mail: yablokov@ifmpan.poznan.pl.
[†] Institute of Molecular Physics.
[‡] Freie Universität Berlin.

(1) Anderson, P. W. In *Magnetism;* Rado, G. T., Shuhl, H., Eds.; Academic: New York, 1963; Vol. 1, Chapter 2.
(2) Zener, C. *Phys. Rev.* **1951**, *82*, 403−405.
(3) Anderson, P. W.; Hasegawa, H. *Phys. Rev.* **1955**, *100*, 675−681.
(4) Blondin, G.; Girerd, J.-J. *Chem. Rev.* **1990**, *90*, 1359−1376.
(5) Blondin, G.; Borshch, S.; Girerd, J.-J. *Comments Inorg. Chem.* **1992**, *12*, 315−340.
(6) Bominaar, E. I.; Borshch, S.; Girerd, J.-J. *J. Am. Chem. Soc.* **1994**, *116*, 5362−5372.
(7) Robert, V.; Borshch, S. A.; Bigot, B. *Chem. Phys.* **1996**, *210*, 401−411.
(8) Borshch, S. A.; Bigot, B. *Chem. Phys. Lett.* **1993**, *212*, 398−402.
(9) Gatteschi, D.; Tsukerblat, B. *Mol. Phys.* **1993**, *79*, 121−143.
(10) Borrás-Almenar, J. J.; Clemente, J. M.; Coronado, E.; Tsukerblat, B. S. *Chem. Phys*. **1995**, *195*, 1−15. Borrás-Almenar, J. J.; Clemente, J. M.; Coronado, E.; Tsukerblat, B. S. *Chem. Phys*. **1995**, *195*, 17−28. Borrás-Almenar, J. J.; Clemente, J. M.; Coronado, E.; Tsukerblat, B. S. *Chem. Phys*. **1995**, *195*, 29−47.



10.1021/ic7006974 CCC: $40.75 
Published on Web 12/11/2007

and their investigation has attracted considerable attention in the past decade.[14]

The theoretical analyses based on the Anderson−Habbard ideas,[4,15] using quantum-chemical DFT and ab initio calculations[16,17] or the parametric solution of exchange and delocalization problem,[9] make a basis for further investigation of the multinuclear mixed-valence clusters. A general theoretical approach to the problem of multinuclear mixed-valence clusters based on the angular momentum technique and successive (chainlike) spin-coupling scheme[18] was proposed.[9,11] The idea of the exchange transfer was introduced[11c,d] into the description of the exchange interactions and electron transfer (interplay and the concept of two kinds of exchange transfer, namely, kinetic and potential ones, was introduced by analogy with basic Anderson's mechanisms of the Heisenberg exchange).[1] Emphasizing the essential success of the theory in consideration of the problem in question, we should draw attention to the fact that the relative values of the theory parameters used for characterization of the compound properties, including the parameters describing Heisenberg exchange, Coulomb interaction, and electron-transfer processes including one-electron and two-electron parts of the total Hamiltonian, can hardly be obtained without experiment. Therefore, the systems permitting the investigation of multinuclear mixed-valence clusters are especially attractive. One class of the systems, which have been intensively investigated in recent years, is molecular polyoxovanadates,[19,20] since they provide a large variety of high-nuclear spin clusters.[21−30] The alkoxo−oxo−vanadium compound $[V_n^{IV}V_{6-n}^{V}O_7(OR)_{12}]^{(4-n)}$ was also shown to be an example of such systems.[31,32] The high symmetry of the cluster molecules, the possibility of changing the valence state of vanadium ions, and the existence of conducting bridges between the ions make them very convenient for the investigation of both the electron transfer and exchange phenomena problems. The effective methodology of the exchange clusters study is facilitated by measurements of their magnetic susceptibility.[33] The temperature-dependent magnetic data quite often can provide insight into the pattern of the cluster energy levels. Electron paramagnetic resonance (EPR) is also known to be a very useful instrument of magnetic clusters investigation, giving information on both isotropic and anisotropic exchange interactions[34−36] and cluster dynamics.[37−39] We have studied the mixed-valence cluster $[V_4^{IV}V_2^{V}O_7(OCH_3)_{12}]$ using EPR and confirmed the decisive influence of the electron transfers on the dynamics of the electron system and structure characteristics of the cluster molecule.[40,41] The present paper reports the EPR study of $[V_4^{IV}V_2^{V}O_7(OC_2H_5)_{12}]$, the ethoxo cluster from the above-mentioned group of oxo−vanadium compounds.

## Results

**Synthesis**. $[V_4^{IV}V_2^{V}O_7(OC_2H_5)_{12}]$ was synthesized according to the procedure previously described.[31] Single crystals of the size and quality suitable for EPR studies were obtained from recrystallization in hexane.

**X-ray Structure Analysis**. The crystal structure of the compound was solved by X-ray diffraction at 295 and 173 K. At room temperature it can be described by a $R\bar{3}m$ space group with the following unit cell parameters: $a$ = 17.5332(15) Å, $c$ = 11.224(2) Å, and $\gamma$ = 120°. The unit cell contains three formula units, and the asymmetric unit comprises one-sixth of the formula unit, i.e., one crystallographic independent vanadium atom.

In each mixed-valence cluster $[V_4^{IV}V_2^{V}O_7(OC_2H_5)_{12}]$ containing four paramagnetic vanadium(+IV) and two diamagnetic vanadium(+V) nuclei, six vanadium nuclei surround an oxo anion, forming a nearly regular octahedron. The vanadium nuclei all equally bind one terminal oxygen


(11) (a) Belinskii, M. I. *Mol. Phys.* **1987**, *60*, 793−819. (b) Girerd, J. J.; Papaefthymiou, v.; Surerus, J.-J.; Munck, E. *Pure Appl. Chem.* **1989**, *61*, 805−811. (c) Borrás-Almenar, J. J.; Coronado, E.; Georges, R.; Palii, A. V.; Tsukerblat, B. S. *Phys. Lett. A* **1996**, *220*, 342−350. (d) Borrás-Almenar, J. J.; Coronado, E.; Palii, A.V.; Tsukerblat, B.S.; Georges, R. *Chem. Phys.* **1998**, *226*, 231−251.

(12) Duclusaud, H.; Borshch, S. A. *J. Am. Chem. Soc*. **2001**, *123*, 2825−2829.

(13) Suaud, N.; Gaita-Ariño, A.; Clemente-Juan, J. M.; Sánchez-Martin, J.; Coronado, E. *J. Am. Chem. Soc.* **2002**, *124*, 15134−15140.

(14) Gatteschi, D.; Sessoli, R.; Villain, J. *Molecular Nanomagnets*; *Mesoscopic Physics and Nanotechnology*; Oxford University Press: Oxford, 2006.

(15) Girerd, J.-J.; Launau, J. P. *Chem. Phys.* **1983**, *74*, 217−226.

(16) Barone, V.; Bencini, A.; Ciofini, I.; Daul, C. A.; Totti, F. *J. Am. Chem. Soc.* **1998**, *120*, 8357−8365.

(17) Guihery, N.; Marlieu, J. P. *J. Chem. Phys.* **2003**, *119*, 8956−8965.

(18) Borrás-Almenar, J. J.; Clemente-Juan, E.; Coronado, E.; Georges, R.; Palii, A. V.; Tsukerblat, B.S.; *J. Chem. Phys.* **1996**, *105*, 6892−6909.

(19) Pope, M. T.; Müller, A. *Angew. Chem., Int. Ed. Engl.* **1991**, *30*, 49.

(20) *Polyoxometalates: from Platonic Solids to Anti-retrovial Activity*; Pope, M. T., Müller, A., Eds.; Kluwer Academic: Dordrecht, The Netherlands, 1994.

(21) Müller, A.; Krickenmeyer, E.; Penk, M.; Walber, H. J.; Bögge, H. *Angew. Chem., Int. Ed. Engl.* **1987**, *26*, 1045.

(22) Müller, A.; Döring, J. *Angew. Chem., Int. Ed. Engl.* **1988**, *27*, 1721.

(23) Müller, A.; Döring, J.; Kahn, M. I.; Wittenben, V. *Angew. Chem., Int. Ed. Engl*. **1991**, *30*, 210.

(24) Müller, A.; Döring, J.; Bögge, H. *J. Chem Soc., Chem. Commun.* 1991, 273.

(25) Gatteschi, D.; Pardi, L.; Barra, A. L.; Müller, A.; Döring, J. *Nature* **1991**, *354*, 436.

(26) Barra, A.-L.; Gatteschi, D.; Pardi, L.; Müller, A.; Döring, J. *J. Am. Chem. Soc.* **1992**, *114*, 8509.

(27) Gatteschi, D.; Pardi, L.; Barra, A.-L.; Müller, A. *Mol. Eng.* **1993**, *3*, 157.

(28) Chiorescu, I.; Wernsdofer, W.; Müller, A.; Bögge, H.; Barbara, B. *Phys. Rev. Lett.* **2000**, *84*, 3454.

(29) Chiorescu, I.; Wernsdofer, W.; Müller, A.; Miyashita, S.; Barbara, B. *Phys. Rev. B: Condens. Matter Mater. Phys.* **2003**, *67*, 020402(R).

(30) Tsukerblat, B.; Tarantul, A.; Müller, A. *J. Chem. Phys.* **2006**, *125*, 054714.

(31) Spandl, J.; Daniel, C.; Brüdgam, I.; Hartl, H. *Angew. Chem., Int. Ed.* **2003**, *42*, 1163−1166.

(32) Daniel, C.; Hartl, H. *J. Am. Chem. Soc.* **2005**, *127*, 13978−13987.

(33) Tsukerblat, B. S.; Belinskii, M. I. *Magnetochemistry and Radiospectroscopy of Exchange Clusters*; Shtinitsa: Kishinev, 1983.

(34) Yablokov, Yu. V.; Voronkova, V. K.; Mosina, L. V.; *Paramagnetic Resonance of Exchange Clusters*; Nauka: Moskow, 1988.

(35) Barra, A.-L.; Gatteschi, D.; Tsukerblat, B. S.; Döring, J.; Müller, A.; Brunel, L.-C. *Inorg. Chem.* **1992**, *31*, 5132−5134.

(36) Gatteschi, D.; Tsukerblat, B. S.; Barra, A.-L.; Brunel, L.-C.; Müller, A.; Döring, J. *Inorg. Chem.* **1993**, *32*, 2114−2117.

(37) Borshch, S. A.; Kotov, I. N.; Bersuker, I. B. *Chem. Phys. Lett.* **1984**, *111*, 264−270.

(38) Polinger, V. Z.; Chibotaru, L. F.; Bersuker, I. B. *Mol. Phys.* **1984**, *52*, 1271.

(39) Voronkova, V. K.; Mrozinski, J.; Yablokov, Yu. V.; Z. *Phys. Chem.* **1997**, *201*, 181.

(40) Augustyniak-Jabłokow, M. A.; Borshch, S.; Daniel, C.; Hartl, H.; Yablokov, Yu. V. *New Chem. J*. **2005**, *29*, 1064−1071.

(41) Yablokov, Yu. V.; Augustyniak-Jabłokow, M. A.; Borshch, S.; Daniel, C.; Hartl, H.; *Acta Phys. Pol., A* **2005**, *108*, 271−281.

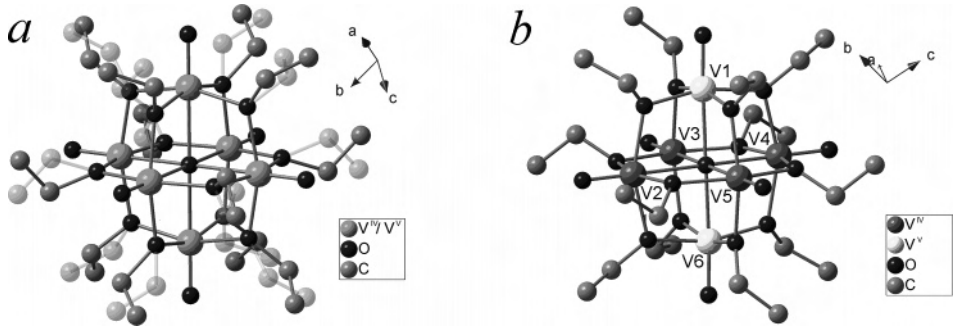


**Figure 1.** Location of the $V^{IV}-V^{V}$ atoms in $[V_4^{IV}V_2^{V}O_7(OC_2H_5)_{12}]$ at 295 K (a) and 173 K (b) determined by valence sum calculations.[32]

**Table 1.** Selected Bond Lengths (Å) and Angles (deg) for $[V_6O_7(OC_2H_5)_{12}]$ at 295 and 173 K (averaged Values Are Shown for Some Bonds)

| | $V-O_{apic}$ | $<V-O_{pl}>$ | $V-O_{centr}$ | $<V-O_{bridge}-V>$ | $<V-O_{centr}-V>$ |
|---|---|---|---|---|---|
| at 295 K | 1.5770 | 1.9775 | 2.2939 | 110.22 | 90 |
| at 173 K | | | | | |
| for $V_1$ ($V_6$) | 1.5913 | 1.9275 | 2.2553 | 109.29 | 90 |
| for $V_2$ ($V_4$) | 1.5990 | 2.0134 | 2.3299 | <111.13> | 90 |
| for $V_3$ ($V_5$) | 1.6020 | 2.0078 | 2.3077 | | |
| | | <2.0106> | <2.3189> | | |

**Table 2.** Valence Sum Calculations for the Crystallographically Independent Vanadium Atoms in $[V_6O_7(OC_2H_5)_{12}]$ Based on X-ray Crystallographic Data Collected at 173 K

| | | | | bond-valence sums | | |
|---|---|---|---|---|---|---|
| compound | $V^{IV}$ | $V^{V}$ | | V(1) | V(2) | V(3) |
| $[V_6O_7(OC_2H_5)_{12}]$ | 4 | 2 | $V^{IV}$ | *4.03* | 4.68 | *4.06* |
| | | | $V^{V}$ | 4.24 | *4.93* | 4.28 |

atom and four $\mu_2$-bridging ethoxo ligands, respectively. The valence sum calculations lead to a conclusion that at room temperature four $V^{IV}$ and two $V^{V}$ valences are equally distributed among six vanadium atoms of the cluster's hexanuclear core (Figure 1a). The room-temperature structure is also characterized by the disorder of the ethyl groups, which all are distributed between two possible conformations.

On cooling, the crystal structure of $[V_6O_7(OC_2H_5)_{12}]$ changes to monoclinic with the $P2_1/n$ space group at 173 K with $a = 10.338(4)$ Å, $b = 17.760(8)$ Å, $c = 11.002(5)$ Å, and $\beta = 106.408(8)°$, with two formula units in the unit cell. The structural parameters of $VO_6$ complexes also undergo change. The hexavanadate core becomes distorted, though the molecule maintains the center of symmetry so that $VO_6$ remain equivalent by pairs (Figure 1b). (We shall distinguish the $V_iO_6$ octahedrons in the equatorial ring of the cluster molecule as $i = 2-5$ and the pole ones as $i = 1, 6$. Let us choose in each $V_iO_6$ group the $O_{central}-V_i-O_{apical}$ direction, and let us call the bonds to the other oxygen atoms from this group deviated from this direction plane bonds. Selected bond lengths and angles of $[V_6O_7(OC_2H_5)_{12}]$ measured at 295 and 173 K are listed in Table 1. We point out that at 295 K all the plane $V_i-O$ bonds are almost identical: their mean value is equal to 1.9775(4) Å. With decreasing temperature, the plane bond lengths in the equatorial $V_{2-5}-O_6$ arrangement increase ($<V_i-O_{pl}>_{equat} = 2.0106$ Å), while in the pole complexes these bonds become shortened ($<V_{1,6}-O_{pl}>_{pole} = 1.9275$ Å). Results of the valence sum calculations[42] for the three crystallographically independent vanadium atoms at 173 K are listed in Table 2.

These data indicate that the $V^{IV}$ valencies are localized and that their arrangement corresponds to the one found in the crystal structure of $[V_6O_7(OCH_3)_{12}]$, i.e., the $V^{IV}$ valences occupy the cluster's equatorial $V_4O_4$ ring[32] (Figure 1b). Let us note that according to EPR results, such a localization should be treated as preferable.

**EPR Measurements.** An X-band EPR study of $[V_4^{IV}V_2^{V}O_7(OC_2H_5)_{12}]$ single crystals was performed on a RADIOPAN spectrometer in the 295−4.2 K temperature interval. The size of the crystals selected did not exceed $0.4 \times 0.4 \times 0.2$ mm, which made it difficult to establish their precise orientation in the resonant cavity. Inaccuracy of the crystals positioning can be estimated as about 5−10°.

For the EPR study, the crystal was oriented in such a way that at room temperature the rotation axis, perpendicular to the direction of the constant magnetic field $\boldsymbol{B}$, was parallel to the [111] direction of the trigonal lattice (at 170 K the rotation axis corresponded to the $[01\bar{1}]$ direction of the monoclinic lattice).

The room temperature (293 K) spectrum consists of a single symmetric signal (we will name it the predominant signal; it is observed at all temperatures in the vicinity of 325 mT, its $g$ factor for different orientations of the crystal is ~1.970−1.985) and the extended signal, evidently visible at magnetic fields of 260−290 *mT* (Figure 2). Figure 2 shows that the extended signal (spectrum) changes with decreasing temperature; however, it is evidently present down to about 140 K. Then its observation becomes difficult, and it appears again below ~45 K when it appears as a single wide EPR line, with the peak intensity comparable to that of the predominant signal.

The angular dependence of the line width of the predominant signal $\Delta\boldsymbol{B}$ at 293 K is repeated with a nearly 90° period and a small change of $\Delta\boldsymbol{B}$ value, from 38 mT to ~34 ± 1 mT (Figure 3). The deviation of the $\Delta\boldsymbol{B}(\theta)$ dependence from the regular form is probably a consequence of the inaccuracy in the weak and broad signals measurements and their superposition with the unresolved signals of the extended spectrum. Cooling to 170 K results in remarkable changes: The $\Delta\boldsymbol{B}$ anisotropy increases starting at about 200 K, and at 170 K, two maxima take different values; the higher is ~47 mT at $\theta = 0°$ (180°), while the lower is $\Delta\boldsymbol{B}$ ~35 mT, at

(42) Brese, N. E.; O' Keeffe, M. *Acta Crystallogr., Sect. B* **1991**, *47*, 192−197.

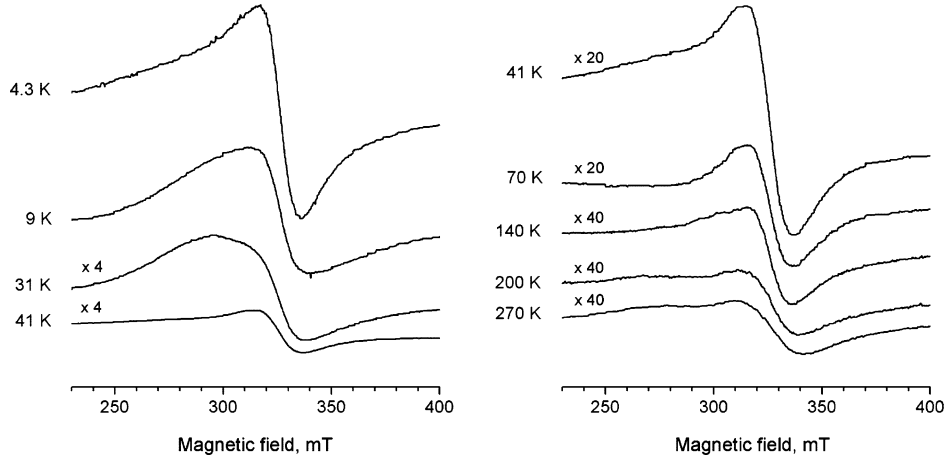


**Figure 2.** Temperature dependence of the EPR spectrum recorded for magnetic field ***B*** parallel [01$\bar{1}$] to the low-temperature structure of the $[V_4^{IV}V_2^{V}O_7(OC_2H_5)_{12}]$ crystal.

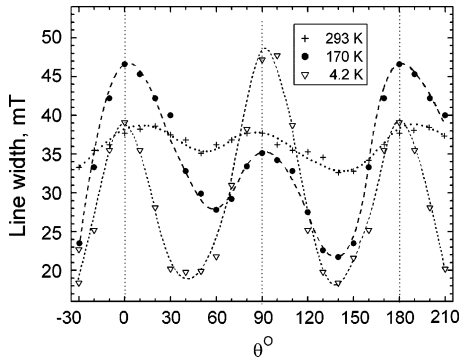


**Figure 3.** Angular dependencies of the $\Delta \boldsymbol{B}$ line width at 293, 170, and 4.2 K. The magnetic field is rotated around the [01$\bar{1}$] direction of the low-temperature phase corresponding to the [111] direction of the trigonal phase. At 170 K, the direction of the magnetic field corresponding to the angle of 0° is close to the [012] crystallographic direction of the low-temperature structure, while for the angle of 90° it is close to the [20$\bar{1}$] direction.

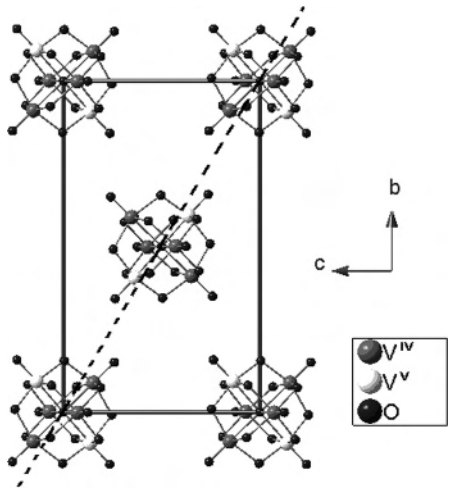


**Figure 4.** Unit cell projection of the low-temperature phase along axis *a*. The dashed line shows the rotation axis.

$\theta = 90°$. There are also two local minima at $\theta \sim 60°$ and $\theta \sim 130°$ of $\Delta \boldsymbol{B} \sim 28$ mT and $\sim 23$ mT, respectively. Such dependence can be understood if we take into account that at 170 K, according to the X-ray data, the four $d^1$ electrons are localized in the equatorial plane of the $V_6$ cluster.

The two sets of magnetically nonequivalent $V_4^{IV}V_2VO_7(OC_2H_5)_{12}$ clusters are present in the compound structure (the unit cell of the compound at 170 K is shown in Figure 4). The equatorial plane of $V^{IV}$ ions of one set of clusters and the normal to such a plane of the second clusters set are nearly parallel to the [01$\bar{1}$] direction of the monoclinic lattice.

The experimental signal is a result of overlapping of the signals from the two types of clusters, declined at a different degree to the [01$\bar{1}$] direction. (The largest separation of these signals due to *g* factor anisotropy amounts to 2.5 mT. It is clear that with a line width of several 10s of mT, the signals cannot be resolved). The angular dependence of the EPR line width of the first set of clusters can be described by $(3 \cos^2 \theta - 1)$ with a maximum at $\theta = 0°$ (180°), two minima at $\theta = \pm 54.74°$, and an additional local maximum at $\theta = 90°$. The angular dependence of the EPR line width of the second set of clusters shows maxima for the directions of ***B*** crossing the $V^{IV}$ localization plane and minima at 90° from this direction. The shift between $\Delta \boldsymbol{B}$ of the maxima of the first set of clusters and the maximum and minimum $\Delta \boldsymbol{B}$ values of the second set, of about ∼15°, gives the asymmetric angular dependence shown in Figure 3.

Let us consider the behavior of the EPR spectrum in the interval 40−4.2 K on increasing temperature.

The presence of two lines in the EPR spectrum in this temperature range is evident. Its fitting by two Lorentzian curves does not present any difficulties for the spectra observed up to 15 K (see Figures 2 and 5); however, with increasing temperature the coincidence of experimental and theoretical curves becomes worse: a little distortion of the broad line shape was probable and overestimated *g* factor values are required for these signals. So, we have limited our analysis to the spectrum at 31 K. We have analyzed the contributions of $S = 1$ and $S = 2$ signals to the observed spectrum. The best fit of the relative intensity of the signals $I_i$ and their ratios, widths, and *g* factors (effective *g* factors for $T \geq 20$ K) are shown in parts a−c of Figure 6. With increasing temperature, both $I_{narrow}$ and $I_{broad}$ decrease and the ratio $I_{broad}/I_{narrow}$ increases (this being true at least up to 20−25 K). In this range of temperatures (40− 4.2 K), the broader signal is more intense than the narrower one (we keep in mind the term "predominant" for the narrower

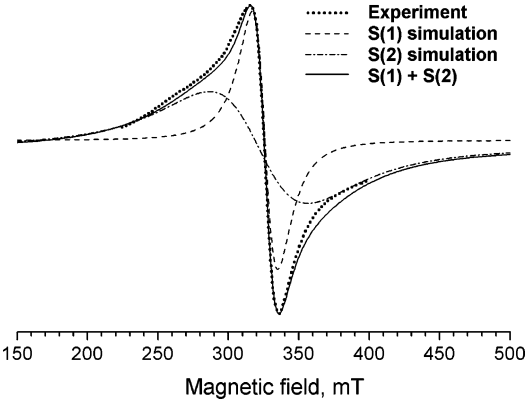


**Figure 5.** Best fit of the theoretical lines to the experimental signal registered at 4.3 K.

signal), then the intensity of the former sharply decreases in the 30−40 K interval and becomes hardly detectable for $T > 40$ K. The presence of this signal could only be inferred from a distortion of the low-field wing of the predominant signal. The $\Delta\boldsymbol{B}(T)$ value of the broader line increases with temperature, whereas the line width of the predominant signal does not noticeably change up to 150 K. Interesting peculiarities of the $\Delta\boldsymbol{B}(\theta)$ dependence of the predominant signal have been observed in the temperature range of 4.2−170 K. They are shown in Figure 7 and reveal that at 4.2 K the positions of the local maxima have been reversed relative to those in the angular dependence at 170 K. The character of $\Delta\boldsymbol{B}(\theta)$ dependence at 4.2 K remains unchanged up to 31 K; however, near 44 K it changes so that both maxima in the resonance line width become of comparable value. With increasing temperature, their ratio changes to reach values characteristic of higher temperatures.

Let us now summarize the experimental results obtained by an EPR study of the $[V_4^{IV}V_2^{V}O_7(OC_2H_5)_{12}]$ cluster, which demand understanding and explanation.

A crucial point for the mixed-valence cluster is the relation between Heisenberg exchange and electron-transfer phenomena. It is important to realize whether the simple isotropic exchange approach is appropriate for understanding the main features of experimental manifestations of the compound properties or the real interplay between these phenomena should be exploited. We assume that the nature of ground energy levels and EPR at the lowest temperatures should first be understood to give the answer. EPR spectra at intermediate temperatures also show interesting features connected with both predominant and extended signals behavior. So, we shall concentrate on the direct and indirect conclusions, which can be drawn on the basis of the analysis of (a) the reasons for observation of EPR at room- and liquid helium-temperatures, as well as the coexistence of the predominant and extended signals in the entire temperature range; (b) the nature of the observed predominant and extended EPR signals and their temperature dependence; (c) the nature of the angular dependencies of the line width of the predominant EPR signal and their change with temperature; and (d) the transformations of the extended spectrum with temperature in the 300−4.2 K range.

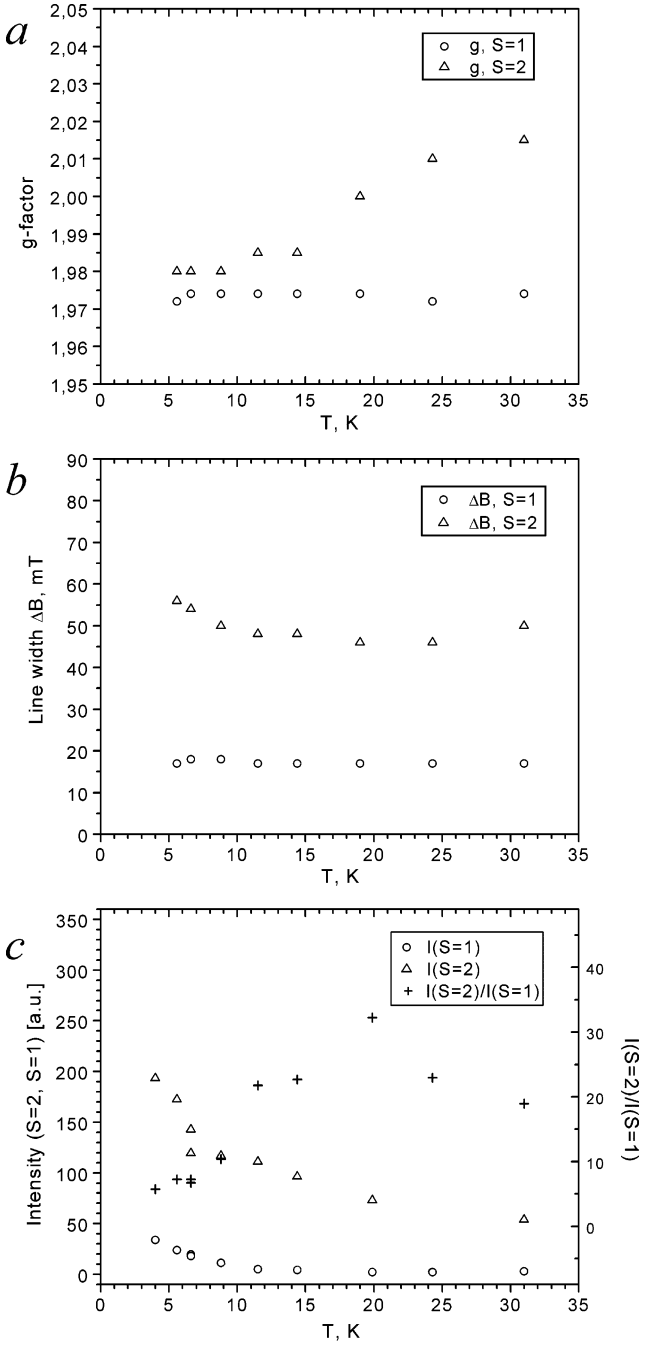


**Figure 6.** Temperature dependencies of the parameters of the fitted lines: (a) $g$(T), (b) $\Delta\boldsymbol{B}$(T), and (c) integral intensities and their ratio.

## Discussion

An individual $V^{IV}$ ion has the $3d^1$ electron configuration and the electron spin $S = {}^1/_2$; the ground term is $^2D$. The nuclear spin of vanadium is $I = {}^7/_2$; however, the hyperfine structure is not expected to be observed in a cluster of four magnetic ions due to a small value of hyperfine splittings ($A_{\text{individ}}$ is about[43] 0.0160 $cm^{-1}$ and $A_{\text{clust}} \approx 0.004$ $cm^{-1}$) and a relatively large width of the observed EPR line (47−20 mT). We have collected[40] information about EPR spectra parameters for the $V^{IV}$ ion surrounded by oxygens in some

(43) Al'tshuler, S. A.; Kozyrev, B. M. *Electron Paramagnetic Resonance in Compounds of Transition Elements*, 2nd ed.; Wiley: New York, 1974.

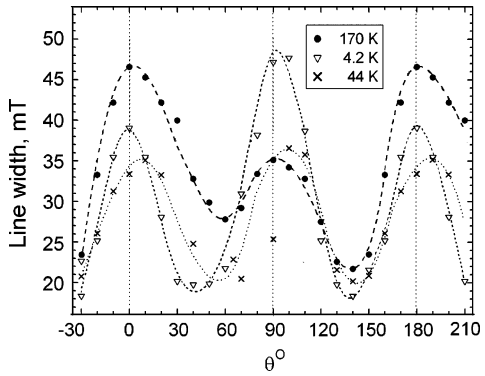


**Figure 7.** Angular dependencies of the effective line width at 170, 44, and 4.2 K. Magnetic field is rotated around the [01$\bar{1}$] direction of the low-temperature phase. The coordination system is the same as that in Figure 3.

compounds, such as $Al_2O_3$, $TiO_2$, $GeO_2$, $V_2O_5$, and binary sulfates, to better understand the electronic properties of the individual $V^{IV}O_6$ unit. The values of the spectroscopic splitting factor $g$ and of the hyperfine structure parameter $A$ depend on the relationship between the values of $^2$D term splitting in the cubic ligand field $\Delta$, the splitting of the ground orbital triplet $\delta$ by the ligand fields of lower symmetry, and the spin-orbital parameter $\lambda$ (the $\lambda$ value for the free $V^{IV}$ ion is $\approx$ 250 $cm^{-1}$) and can change in a relatively large interval.[40,43] The $\delta$ value also determines the conditions of the EPR observation. In the high-symmetry ligand field, the strong spin−orbit coupling efficiently mixes the lowest $d_{xy}$ orbital of the $^2$T triplet (occupied by a $3d^1$ electron) and the upper orbitals and leads to relaxation times so short that EPR is only observable at very low temperatures. In $[V_4^{IV}V_2^{V}O_7(OCH_3)_{12}]$ and $[V_4^{IV}V_2^{V}O_7(OC_2H_5)_{12}]$, however, the EPR signals are observed without difficulties even at 300 K. This supposes the presence of the strong noncubic ligand field component on the vanadium ion. Results of the structural study of the studied compound substantiate this supposition. The bond lengths V−O, involving the bridging oxygens-(see Table 1), are typical for the metal ion−oxygen $\sigma$ bonds (1.9775−2.0134 Å). At the same time, the terminal oxygen bond lengths (1.5770−1.6020 Å) are typical for double covalent bonds with oxygen in vanadyl $VO^{2+}$ complexes. The distances to the sixth, central oxygen atom are much longer (2.2939−2.3299 Å). This displacement of the vanadium atom from the octahedron's central positions is characteristic for polyoxometalates and vanadium oxides. All these data support the idea that the vanadium ions are present as $VO^{2+}$ ions.

Valence sum analysis of X-ray data leads to a conclusion[32] (see Table 2) that the four unpaired electrons, equally distributed among the six vanadium ions of the mixed-valence cluster $[V_4^{IV}V_2^{V}O_7(OR)_{12}]$ studied at room temperature, are localized on vanadium ions of the clusters' equatorial $V_4O_4$ ring at 173 K. One can consider the change in distribution of the extra electrons on vanadium ions as a manifestation of electron transfer. Let us recall that at temperature lowering, change in the crystal symmetry takes place. Although the phase transition is rather important, as it leads to localization of the $V^{IV}$ ions, no abrupt changes (appearance of singularities or signal intensity change) are detected in the EPR spectra in the temperature interval of 293−173 K. This observation allows a supposition that the electron transfers evident in high temperatures occur in lower temperatures, as well. We shall prove that the transfer of electrons determines the main features of the observed EPR spectra in the whole temperature range, including peculiarities in the behavior of the broadened signals and changes in the angular dependencies of line width $\Delta \boldsymbol{B}(\theta)$ of the predominant signal.

Though, as mentioned in the Introduction, a number of a thorough theoretical investigations of the mixed-valence systems are available, the problem of the coexistence of the Heisenberg exchange and the exchange transfer in a more complex system such as the one under study demands a special theoretical analysis. We shall apply here a very simple phenomenological approach, based on a consecutive account of the effects, which seem to be important. We begin with the consideration of the isotropic Heisenberg exchange interaction in the possible configurations of four $V^{IV}$ ions, then consider consequences of the account of electron transfers for the system of six ions − four electrons and mixing of the arising equivalent configurations, emphasizing the moments, which facilitate an understanding of the observed phenomena.

For interpretation of the EPR spectra, the model with the preferable localization of the unpaired electrons on the four equatorial V ions (Figure 1b) is assumed, which permits a correct interpretation of the X-ray data at 173 K. The complete delocalization of additional electrons, which is revealed by X-ray data of $[V_4^{IV}V_2^{V}O_7(OC_2H_5)_{12}]$ at 293 K, can be treated as proof of existence of the three equivalent localizations of the four $d^1$ electrons on vanadium ions in the three planes of the $V_6$ core and the transitions between these possible $V_4^{IV}$ configurations (see later).

The $d^1$ electrons are involved at 173 K in the exchange interactions described by the Hamiltonian

$$H_{ex} = J_1(S_2S_4 + S_3S_5) + J(S_2S_3 + S_3S_4 + S_4S_5 + S_5S_2) \quad (1)$$

This Hamiltonian together with the terms $H_z$, $H_{fs}$, and $H_{hfs}$, describing the interactions of the vanadium ions with the magnetic field, zero-field splitting of the states of the total spin $S$, and the hyperfine interactions of electron and nuclear magnetic moments of vanadium (whose nuclear spin $I_i = {}^7/_2$), respectively, lead to the spin Hamiltonian

$$H = H_{ex} + H_z + H_{fs} + H_{hfs} \quad (2)$$

which should describe the EPR spectrum. In eq 1, $S_i = {}^1/_2$ (the index in $S_i$ corresponds to the notation of the vanadium ions in Figure 1b) and $J_1$ and $J$ are the parameters of the isotropic exchange interactions between the $V^{IV}$ ions denoted in Figure 1b. The total spin $S$ of the cluster is obtained according to quantum mechanical rules, which consist of adding up the individual spins via the $S_{24}$ and $S_{35}$ intermediates. The individual, intermediate, and total spin operators in eq 1 commute, leading to the solution of the exchange Hamiltonian:

$$\frac{E}{|J|} = \frac{J_1}{2|J|}[S_{24}(S_{24}+1) + S_{35}(S_{35}+1) - 3] + \frac{J}{2|J|}[S(S+1) - S_{24}(S_{24}+1) - S_{35}(S_{35}+1)] \quad (3)$$

The set of spin states consists of one quintet ($S = 2$), three triplets ($S = 1$), and two singlets ($S = 0$). The signs and values of the $J_1$ and $J$ parameters determine the relative energies of the total spin states and can be instructively presented in the form of the so-called correlation diagram (Figure 8).

The correlation diagram can describe both antiferro- and ferromagnetic (a.f.m. and f.m.) interactions between $V^{IV}$ ions. According to the exchange Hamiltonian (eq 1) form accepted, the lowest states having the total spin $S = 0$ correspond to the antiferromagnetic interactions for $J > 0$. The unpaired electron occupies the $d_{xy}$ orbital (in the local coordinate system), and there are two channels for the indirect exchange interactions between $V^{IV}$ ions. The interaction through the pure p orbital of the oxygen of $OC_2H_5$ group is expected to have, in accordance with the Goodenough−Kanamori rules,[44] the antiferromagnetic nature. The interaction of the neighboring $V^{IV}$ ions through the orthogonal p orbitals of the central O atom should be ferromagnetic. On the basis of the experimental data, we can draw conclusions about the results of the competition between interactions of different types.

The character of the EPR signals (spectra) of the cluster is determined by two total spin states with $S = 1$ and $S = 2$. They both should be described by the spin Hamiltonian of eq 4 (the tetragonal symmetry of the $V_4^{IV}V_2^{V}$ configuration of the cluster is accepted, and all symbols are conventional):

$$H = \{g\}\beta BS + D\left[S_z^2 + \frac{1}{3}S(S+1)\right] + \{A\}IS \quad (4)$$

Magnetic states with $S = 1$ and $S = 2$ should already be split in the absence of the magnetic field. However, the fine structure of these spin states (as well as the hyperfine structure) is not observed, and instead, signals of two types appear: a single symmetrical signal with line width $\Delta \boldsymbol{B} \sim$ (20−47) mT, $g$ factor values 1.97−1.99 and a broad extended signal whose shape is temperature dependent. As we described in the previous paragraph and showed in Figure 2, in the temperature range of 293−140 K, the broad signal looks like an unresolved spectrum and then it vanishes to appear again in the narrow temperature interval of ∼40−30 K and is observed down to 4.2 K. Taking into regard the results for the $[V_4^{IV}V_2^{V}O_7(OCH_3)_{12}]$ cluster,[40,41] whose spectrum of four signals corresponding to the $S = 2$ state was observed directly in the range of 293−200 K (see Figure 5 in ref 40 and Figure 2 in ref 41) and transformed into a broad signal at lower temperatures, we attributed the extended signal in the spectrum of $[V_4^{IV}V_2^{V}O_7(OC_2H_5)_{12}]$ to the unresolved fine structure of the EPR spectrum of the $S = 2$ state. The absence of resolution of this spectrum at high temperatures and its changes with the temperature lowering lead to a conclusion that certain dynamic processes have to take place, resulting in the averaging of the expected fine structure spectrum. Similarly, the relatively narrow predominant signal should be ascribed to the $S = 1$ states, whose fine structure is also averaged. The large size of the peripheral fragments of the cluster molecules and the absence of contacts between vanadium ions of different molecules allow one to ignore the intermolecular exchange interactions as a possible mechanism of spectra averaging. The changes of the spectrum shape with temperature support this conclusion. This means that such averaging should be connected with the intracluster dynamics, and we shall now show that this dynamic is determined by the transitions of the unpaired electrons between the $V^{IV}$ and $V^{V}$ ions leading to different configurations of the mixed-valence cluster.

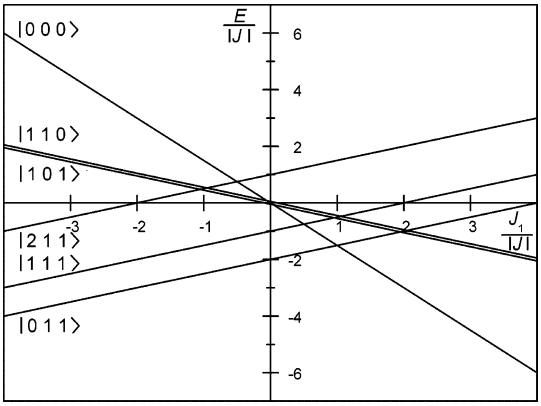


**Figure 8.** Energy of the spin states $E|S,S_{24},S_{35}\rangle$ of the cluster in units of $|J|$ as a function of $J_1/|J|$ according to eq 3.

The correlation diagram, corresponding to eq 3, shows that for any ratios between the values and signs of $J_1$ and $J$ the lowest energy states are the states of $S = 0$ (for $J > 0$, a.f.m. exchange) or of $S = 0$ and $S = 2$ (at $J < 0$, f.m. exchange). A remarkable feature of the $[V_4^{IV}V_2^{V}O_7(OC_2H_5)_{12}]$ cluster as well as of the $[V_4^{IV}V_2^{V}O_7(OCH_3)_{12}]$ cluster studied earlier[40,41] is the fact that both narrow (from $S = 1$ states) and broader (from $S = 2$ state) EPR signals are simultaneously observed in the whole temperature range down to liquid helium temperatures, with the intensity of the total spectrum being a sum of the signals from $S = 1$ and $S = 2$ increasing on temperature decreasing to 4.2 K. This shows that the $S = 1$ and $S = 2$ states are the lowest and have comparable energy. We should mention that the correlation diagram shown in Figure 8 permits the $S = 1$ and $S = 2$ states to be in close vicinity when $J < 0$ and $J_1/|J| \approx -1$; however, these states are not the lowest states in this case. It means that the isotropic exchange interactions in the form of eq 1 cannot explain the experiment and the transfers of the $V^{IV}$ d electrons on the empty $V^{V}$ orbitals should be taken into consideration.

It is convenient to start again with the configuration of $V^{IV}$ ions in the cluster at 173 K. The valence-sum calculations indicate (see Table 2) that four paramagnetic vanadium (+IV) ions are arranged in an equatorial fashion (Figure 1b). These calculations are based on the X-ray crystallographic data, which directly demonstrate a lengthening of all V−O bond lengths in equatorial $VO_6$ units in comparison with the

(44) Goodenough J. *Magnetism and the Chemical Bond*; Interscience: New York, 1963.

pole ones (Table 1). An increase of V−O bond lengths in magnetic complexes is due to weakening of chemical bonds by negatively charged electrons located on the antibonding orbital. At the same time, one can expect that delocalization of unpaired electrons at room temperature should equalize the bond lengths. The observed structural changes as well as the differences in the electron densities on equatorial and pole $VO_6$ units are supposed to be stipulated by distortion of the cluster molecules when the temperature decreases and the crystal symmetry lowers.

In the simple case of two ions in different oxidation states in similar environments, the transfer of the excess electrons between equivalent $M^n - M^{n+1}$ and $M^{n+1} - M^n$ states lead to the doubling of the $S$ levels (and splitting on $\pm P(S + {}^1/_2)$) since the states' mixed-valence pair are doubly degenerated.[2,3] The precise solution of the problem was shown[11] to already vary in trimeric systems as some additional second-order spin-dependent electronic processes, involving three metal sites, should also be considered. The solution for the hexanuclear $[V_4{}^{IV}V_2{}^{V}O_7(OC_2H_5)_{12}]$ cluster is even more complicated, due to the high degree of degeneration (quasi-degeneration) of the spin states, which arises as a consequence of the appearance of a number of equivalent configurations (or configurations of very close energies) of $V^{IV}$ ions. However, the conclusion about splitting of the cluster total spin states as a result of a joint action of both the Heisenberg exchange and the electron transfers remains valid.[9,37] Intervals between these spin levels and their common pattern are now determined by Heisenberg exchange and the independent contributions of the kinetic and potential exchange transfers.[11] The solution of this problem should be a subject of special study. We can make judgments about some of lowest spin levels on the basis of our experimental data. Taking into account these remarks, we shall use the spin Hamiltonian approach to tentatively explain the observed EPR spectra and their transformations with temperature.

Generally speaking, in our starting configuration with four magnetic $V^{IV}$ ions localized in the equatorial plane of the 6V octahedron, 4 unpaired $d^1$ electrons can be distributed between 6 metallic centers in 15 ways. We shall now analyze the transitions of one electron between the equatorial $V^{IV}{}_i$ ($i = 2-5$) ion and one of the pole vanadium ions $V^{V}{}_j$ ($j = 1, 6$) giving rise to eight $(V^{IV}{}_3V^{V})_i(V^{IV}V^{V})_j$ configurations. The environments of the equatorial and pole vanadium ions are characterized by similar structural parameters at temperatures 293−200 K (see Table 1; 200 K is the temperature where the room-temperature character of the angular dependence of the line width $\Delta \boldsymbol{B}(\theta)$, i.e., room-temperature electron distribution, starts to change), and these parameters only change slightly with temperature lowering. The $d_{xy}$ orbitals of all V ions in the equatorial and pole $VO_6$ units are similarly bridged, and we can conclude that the intracluster $V^{IV}{}_4V^{V}{}_2 \leftrightarrow (V^{IV}{}_3V^{V})_i(V^{IV}V^{V})_j$ transitions are allowed from both the energy and the symmetry points of view. As a result, eight mixed doubled configurations of $V^{IV,V}$ ions of the $V^{IV}{}_4V^{V}{}_2-(V^{IV}{}_3V^{V})_i(V^{IV}V^{V})_j$ type are possible, which due to the presence of the small difference in the structure parameters of equatorial $V_iO_6$ units and center of symmetry of cluster molecule, form two four-fold degenerated sets of the total spin states with close energy values. It can be assumed that the contributions of the $V^{IV}{}_4V^{V}{}_2$ and $(V^{IV}{}_3V^{V})_i(V^{IV}V^{V})_j$ configurations can be realized with the same probabilities at high temperatures and with slightly different probabilities at temperatures lower than 200 K, with some greater weight from the $V^{IV}{}_4V^{V}{}_2$ contribution.

The account of the electron transfers leads to the splitting (and to a new pattern) of spin multiplets as well as to the mixing of states characterized by the same total spin. The greater the differences in the contributions of the $V^{IV}{}_4V^{V}{}_2$ and $(V^{IV}{}_3V^{V})_i(V^{IV}V^{V})_j$ configurations, the smaller the value of resonance splitting of the mixed configurations. The changes in the new pattern of spin multiplets will also occur due to the dependencies of splittings on the intermediate spin values[11] and on the possible effects stipulated by the degeneration of the spin multiplets.[9] If the resulting effect of the electron transfer is of the same order of magnitude as the exchange parameter $J$, the sequence of the spin levels can be changed and the ground state can have a nonzero spin. As can be seen from the correlation diagram in Figure 8, the lowest $S = 1$ and $S = 2$ states have close energies only in the case when the energy of their stabilization is approximately proportional to $S$ value. It is important that such a situation can occur for $J > 0$ (and only for $J > 0$) in a wide interval of $J_1/|J|$ values. Just this fact stipulates the observed closeness of the energies of $S = 1$ and $S = 2$ states in the $OCH_3$ and $OC_2H_5$ clusters differing by geometry parameters of $V_iO_6$ units.

A transfer of even one electron modifies the arrangement of $V^{IV}$ ions and the picture of exchange splitting of the spin multiples. Therefore, it is necessary to consider the total spin levels pattern arising after the electron transfer.

Exchange interactions in the $(V^{IV}{}_3V^{V})_i(V^{IV}V^{V})_j$ configuration are described by the Hamiltonian of the form

$$H_{ex} = J_1S_2S_4 + J(S_2S_3 + S_3S_4) + J_2(S_2S_1 + S_3S_1 + S_4S_1) \quad (5)$$

The solution of Hamiltonian eq 5 is

$$E = \frac{J_1}{2}[S_{24}(S_{24}+1) - 2S_1(S_1+1)] + \frac{J}{2}[S_{234}(S_{234}+1) - S_{24}(S_{24}+1) - S_1(S_1+1)] + \frac{J_2}{2}[S(S+1) - S_{234}(S_{234}+1) - S_1(S_1+1)]$$

Let $J = J_2$ (this approximation does not disturb a general consideration but makes the analysis more convenient), and then a solution of eq 5

$$\frac{E}{|J|} = \frac{J_1}{2|J|}[S_{24}(S_{24}+1) - 2S_1(S_1+1)] + \frac{J}{2|J|}[S(S+1) - S_{24}(S_{24}+1) - 2S_1(S_1+1)] \quad (6)$$

leads to the correlation diagram shown in Figure 9. For $J > 0$, the exchange interactions (eq 5) determine the structure of the levels of the total spin (eq 6), which is similar to that obtained for the configuration $V^{IV}{}_4V^{V}{}_2$ (eq 1); hence, this consideration proves again that only the single-electron-

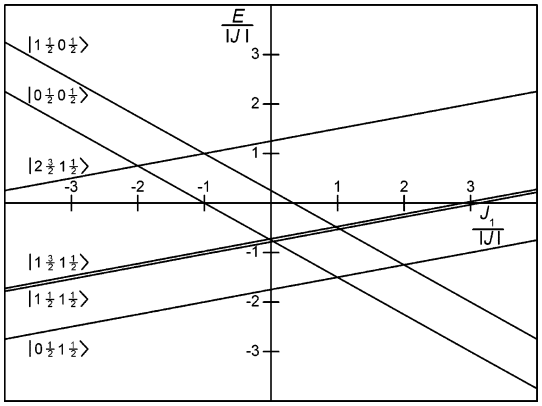


**Figure 9.** Energy of the spin states of the cluster in units of $|J|$ as a function of $J_1/|J|$ according to eq 6.

transfer $V^{IV}{}_4V^V{}_2 \leftrightarrow (V^{IV}{}_3V^V)_i(V^{IV}V^V)_j$ for $J > 0$ leading to the mixed configurations $V^{IV}{}_4V^V{}_2-(V^{IV}{}_3V^V)_i(V^{IV}V^V)_j$ describes the situation when the energies of the lowest states $S = 1$ and $S = 2$ are close. Also, from Figure 9 it follows that for $J < 0$ (f.m. exchange), the Hamiltonian (eq 5) implies that the states of $S = 1$ and $S = 2$ can be the ground states, depending on the ratio of the parameters $|J|$ and $J_1$, so that in certain conditions $E_{(S=1)} \approx E_{(S=2)}$. However, taking into account that (a) ferromagnetic exchange, $J < 0$, cannot explain the observed EPR spectra for $V^{IV}{}_4V^V{}_2$ configuration, (b) the conditions for exchange interactions in $V^{IV}{}_4V^V{}_2$ and $V^{IV}{}_3V^VV^{IV}V^V$ configurations are the same, and (c) it would be impossible to explain the closeness of energies of $S = 1$ and $S = 2$ states in this case, we assume that for both configurations the situation with $J > 0$ is preferable.

We shall now analyze the spectrum observed at 4.2 K and the contributions of the $S = 1$ and $S = 2$ signals to the spectrum for the temperature interval 4.2−31 K (see Figure 6). The intensity of the EPR spectrum is proportional to the magnetic susceptibility of the magnetic centers totality, and we can use the van Vleck type expression[45]

$$I \sim \frac{\sum_S S(S+1)(2S+1)\exp^{(-E(S,S_{ij},S_i,P)/kT)}}{kT\sum_S (2S+1)\exp^{-(E(S,S_{ij},S_i,P)/kT)}} \qquad (7)$$

for the four-nuclear cluster magnetic susceptibility to compare the observed and expected signals behavior. Here, $S_{ij}$ are $S_{24}$ and $S_{35}$ intermediate spins. One should modify the expression of eq 7 by taking into account the transformation of the total spin states due to electron transfers. The whole pattern of the spin levels is unknown; however, only the lowest states of the total spin $S = 1$ and $S = 2$ are populated at very low temperatures, and we shall use eq 7 only for these cases.

The use of eq 7 for $S = 1$ and $S = 2$ shows that the dependencies $I_{S=1}(T)$ and $I_{S=2}(T)$ resemble the experimental ones only in the case when the corresponding energies $E(S,S_{ij},S_i,P)$ are really nearly equal and that only in the case

(45) van Vleck, J. H. *The Theory of Electric and Magnetic Susceptibilities*; Oxford: London, 1932.

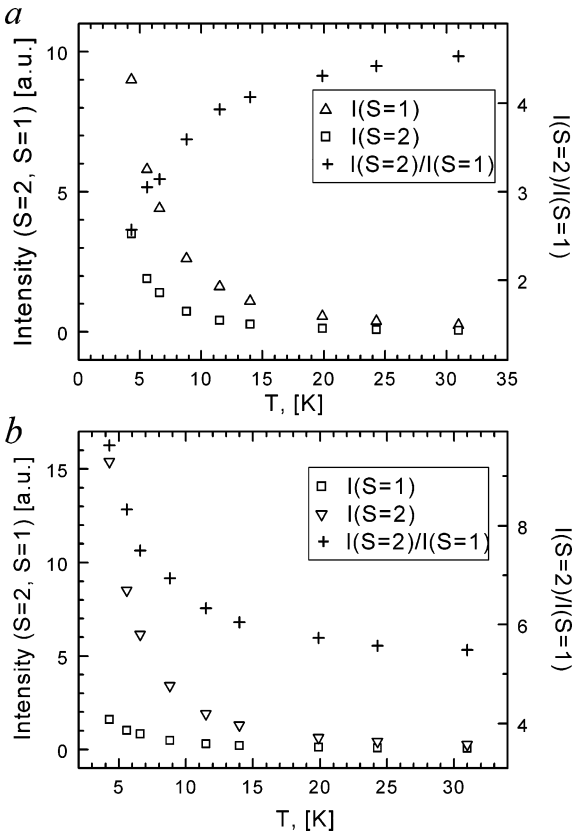


**Figure 10.** Temperature dependencies of the integral intensities $I(S_i)$ of the EPR signals for the states of $S = 1$ and $S = 2$ and their ratios for (a) $E_{(S=2)} > E_{(S=1)}$, $E_{(S=2)} - E_{(S=1)} = 2$ cm$^{-1}$ calculated with eq 7; and (b) $E_{(S=1)} > E_{(S=2)}$, $E_{(S=1)} - E_{(S=2)} = 2$ cm$^{-1}$ calculated with eq 7.

when $E_{S=2} > E_{S=1}$ corresponds to the increase in the $I_{S=2}/I_{S=1}$ ratio with temperature. It has been shown (Figure 10) that the difference $\Delta E = I_{S=2} - I_{S=1}$ is estimated to be about 2 cm$^{-1}$.

The one-jump electron transfers in the studied cluster reorganize the whole system of the total spin energy states. To achieve the situation with $S = 1$ and $S = 2$ states having the lowest energy, the intervals of the splitting of the total spin states should be comparable in magnitude to the exchange parameter $J$ (the splitting of $S = 2$ state should be some more than doubled splitting of $S = 1$ ones). For a reasonable value of $J \sim 100$ cm$^{-1}$, the rate of the spin transition should be about $10^{12}$ s$^{-1}$. An estimation of $J \sim 100$ cm$^{-1}$ was done using the fact that up to temperatures of ~20 K, the fitting of the integral intensity of EPR signals does not show deviation from the van Vleck equation. Moreover, we have seen that EPR also indicates the presence of another process or another type of the spin transition that would average the complicated spectrum of the $S = 1$ and $S = 2$ states to the single EPR line. The two-jump electron transfers $V^{IV}{}_4V^V{}_2 \leftrightarrow (V^{IV}{}_2V^V{}_2)_iV^{IV}{}_2$ or $V^{IV}{}_4V^V{}_2 \leftrightarrow (V^{IV}V^V V^{IV}V^V)_iV^{IV}{}_2$ represent such processes. These transfers change the direction of the symmetry axis of the $V^{IV}{}_4V^V{}_2$ cluster and resemble the Brownian motion of molecules in a liquid.

As it is known, conditions of averaging are stipulated by the ratio between the characteristic rate of dynamics $\tau_c^{-1}$ and

parameter, which should be averaged.[43,46] In our case, a single EPR line is observed while $\tau_c^{-1} \gg 2D/\hbar$ for the $S = 1$ state and $\tau_c^{-1} \gg 6D/\hbar$ for the $S = 2$ state ($D$ is the fine structure parameter), and a well resolved spectrum corresponds to the opposite relation (see Figure 5 in ref 40). In the intermediate case, a blurred spectrum is observed and sometimes it can barely be detected.

Let us accept that the fine-structure parameters $D$ for methyl and ethyl clusters have comparable values and $D_{S=2} \approx D_{S=1}$ to estimate the required rate of the electron transitions $\nu_{tr}$ for the temperatures $T > 140$ K. In $[V_4^{IV}V_2^{V}O_7(OCH_3)_{12}]$ compound $D_{quintet} \approx D_{triplet}$ was shown[40] to be equal $\cong 0.03$ $cm^{-1}$. As the fine structure of the $S = 1$ state is averaged due to electron transitions when $\nu_{tr} > 2\ D_{triplet}/h$, the value $\nu_{tr} = (0.5-0.6) \times 10^{10}\ s^{-1}$ is sufficient for averaging the fine structure of the $S = 1$ states. At the same time, it can be insufficient for averaging the fine structure of the spectrum of the $S = 2$ state, whose whole extension is about 3 times larger than that for the $S = 1$ state, i.e., about 0.18 T. Such a situation takes place[40] for $[V_4^{IV}V_2^{V}O_7(OCH_3)_{12}]$ at the temperature interval of 293−200 K.

Let us recall that the greater the differences in the $V_iO_6$ unit geometry the greater the differences in the probability of finding unpaired electrons on the equatorial and pole $V_iO_6$ positions and the lower the transfer frequency. For example, the difference in the geometrical parameters of $V_iO_6$ units in the methoxy−$V_4V_2$ cluster at 290−250 K is larger than that in the ethoxy−$V_4V_2$ one. In agreement with this, in the latter case the transition frequencies are higher and can average the fine structures of both the $S = 1$ and $S = 2$ (though incompletely) states.

The large width (extent) of the $S = 2$ signal observed for $[V_4^{IV}V_2^{V}O_7(OC_2H_5)_{12}]$ at magnetic fields of 260−290 mT at temperatures of 290−200 K and its blurring below 140 K show that conditions of spectrum averaging are fulfilled incompletely at high temperatures and become broken at temperatures lowered to 70 K. We can only suggest very preliminary reasons for the mentioned spectrum transformations in this temperature region. In accordance with the above consideration, there are many energy states corresponding to the different configurations of vanadium ions and differing by their energies; also, parts of these states are degenerated or quasi-degenerated. The frequencies of transitions between configurations depend on distinctions of their energies and can noticeably differ. Thus, the observed EPR signals originate from the large number of $S = 1$ and $S = 2$ states, which are only populated in the considered temperature interval and can differ by their parameters and internal dynamics of the cluster. Taking into account the presence of the degenerations, one can expect manifestations of some vibronic instability and of temperature dependence of EPR signals. Mentioned factors are difficult to analyze quantitatively; however, they can evidently influence the conditions of EPR observation. We shall now consider two results supporting these conclusions. The first is connected with peculiarities of the angular dependence of the line width of the $S = 1$ signal at different temperatures and the second with the temperature dependence of the observation conditions of the $S = 2$ line, which has the Lorentzian shape in the interval 4.3−31 K, disappears above 40 K, and reappears as the expanded spectrum at high temperatures.

The most significant contribution to the line width of the predominant signal is determined by the averaged fine and hyperfine structures of the EPR spectra. (Let us mention that the conditions of the complete averaging are fulfilled for this signal at all temperatures and for all crystal orientations.) An extension of both the fine and hyperfine patterns of the spectrum strongly depends on the orientation of the crystal in the magnetic field. Accordingly, the line width also depends on the orientation. The $\Delta\boldsymbol{B}$ anisotropies due to fine and hyperfine structures have symbate character: their extension is maximum in the parallel orientation of the magnetic field and symmetry axis of the cluster ($\theta = 0°$) and larger than that observed for $\theta = 90°$. An interesting feature of the angular dependence of fine structure splitting is its value of to zero for $\theta = 54.74°$, indicating the (3 $\cos^2\theta - 1$) character of $\Delta\boldsymbol{B}(\theta)$ dependence and resulting in the narrowest line width for this orientation of the crystal. This character of the $\Delta\boldsymbol{B}(\theta)$ dependence is observed for the compound in question for $T \leq 170$ K, which confirms the correct understanding of the nature of observed signals and $\Delta\boldsymbol{B}(\theta)$ dependence. In the range of 293−210 K, the direction $V_{i\ pole}-O_{centr}-V_{j\ pole}$ is different for different configurations, depending on the electron transfers; however, the cluster orientation in different configurations implies that these different directions are mutually perpendicular. Hence, if the magnetic field is applied along the $V_{i\ pole}-O_{centr}-V_{j\ pole}$ direction of one configuration it is perpendicular to the $V_{i\ pole}-O_{centr}-V_{j\ pole}$ direction of another configuration. (We analyzed the averaged configurations appearing as a result of the two-jump transitions between configurations of the $V_4^{IV}V_2^{V}-V_3^{IV}V^{V}V^{IV}V^{V}$ type.) As a result, the EPR line widths corresponding to $\theta$ values equaling 0° and 90° are determined by the contributions of the averaged largest and smallest fine and hyperfine splittings simultaneously. We note that observation at 293 K of the smallest $\Delta\boldsymbol{B}$ value for $\theta \cong 45°$ is an argument for the concept of three equally probable $V^{IV}_4$ configurations.

An increase in the $\Delta\boldsymbol{B}(\theta)$ anisotropy and the fact that for $\theta = 0°$ and 90° $\Delta\boldsymbol{B}$ takes different values confirms a conclusion on the preferred localization of $V^{IV}$ ions in the four equatorial positions at temperatures from 170 to ∼210 K. The change in the relative $\Delta\boldsymbol{B}(\theta)$ values at 170 and 4.2 K allows a conclusion that the change in the preferred $V^{IV}$ ions localization occurs with temperature lowering. At 170 K, they occupy definite equatorial positions, whereas at 4.2 K they are localized in the perpendicular plane. This arrangement remains up to 31 K and begins to change at 44 K. Let us point out that near this temperature the intensity of the averaged $S = 2$ signal changes dramatically. We have discussed above the possible reasons for changes in the rate of dynamical processes taking place in the crystal studied. These changes are accompanied, of course, by the change in the crystal structure, one manifestation of which is the

(46) Anderson, P. W. *J. Phys. Soc. Jpn.* **1954**, *9*, 316.

change of the symmetry axis direction of the cluster molecule, which has the character of the phase transition. This transition is supposed to have a cooperative vibronic nature. The conclusion is supported by the quenching of one of the dynamical degrees of freedom in the critical field and also by its typical deceleration in the vicinity of a critical point. To elucidate this statement, we return to the consideration of the temperature behavior of the $S = 2$ signal in the 4.3−31 K range.

We have mentioned the difficulty of fitting the spectrum for temperatures higher than 15−20 K resulting in some effective overestimated $g$ values for the $S = 2$ EPR line. When the zero-field splitting terms of the spin Hamiltonian are comparable with the Zeeman term and smaller than the microwave quantum $h\nu$ value used, most of the transitions between the $S = 2$ spin levels are grouped in the low-field region of the spectrum,[47] and even minor violation of the complete averaging conditions $\nu_{tr} > nD$ will result in a distortion of the line shape and in a small shift of the envelope of $S = 2$ signal to the low-field region. This observation corresponds to the beginning of the transition from the state of crystal lattice (below 40 K) to another one (above this temperature), due to phonon-induced reasons.

## Conclusion

The decisive facts allowing the elucidation of the nature of the studied mixed-valence $[V_4^{IV}V_2^{V}O_7(OC_2H_5)_{12}]$ cluster compound are the following: the increase of EPR signal (and magnetic susceptibility) with temperature decrease, the closeness of the energies of the ground $S = 1$ and $S = 2$ total spin states (with $E_{S=2} > E_{S=1}$ and $E_{S=2} - E_{S=1} \approx 2$ $cm^{-1}$), the presence of dynamical processes averaging the fine structure of the EPR spectra of these states in some temperature ranges, and the deceleration or breaking of these processes in other intervals of temperature and change in the conditions of localization of the $V^{IV}$ ions with changing temperature.

The $d^1$ electron-transfer phenomena have been shown to be the crucial element needed to solve the problem of this cluster properties. Two types of electron transfers were assumed in the phenomenological model used for explanation of the cluster properties formation: first, the single-jump transfer leading to the formation of the mixed configurations of the $V_4^{IV}V_2^{V}-V_3^{IV}V^{V}V^{IV}V^{V}$ type, doubling and splitting the total spin states, imposed by the Heisenberg−Dirac−van Vleck model of isotropic exchange interactions, and second, the double-jump transfers from the starting $V_4^{IV}V_2^{V}$ configuration or the electron transfers between the $V_4^{IV}V_2^{V}$ and $V_3^{IV}V^{V}V^{IV}V^{V}$ mixed configurations. These types of electron transfers explain the dynamical phenomena naturally, as well as the temperature and angular dependencies of the EPR.

A situation where the $S = 1$ and $S = 2$ total spin states are the lowest and have close energies was also shown to take place for the $[V_4^{IV}V_2^{V}O_7(OCH_3)_{12}]$ cluster studied previously.[19,20] The existence of states with such specific features in the clusters differing in the geometry and exchange parameters can be understood only on the assumption of antiferromagnetic Heisenberg exchange between vanadium ions and of the electron transitions in the mixed-valence centers leading to resonant splittings approximately 2 times larger for the $S = 2$ state than for the $S = 1$ state.

All other properties of the $OCH_3$ and $OC_2H_5$ clusters (the change in the transition rates averaging the EPR spectra and, importantly, the conditions determining the preferred localization of the four $d^1$ electrons changing with temperature) confirm the conclusion on the occurrence of electron transitions. The same conclusion is also supported by the observation of additional instability of the clusters in the temperature interval of 40−140 K, evidencing the structural and spin degenerations in the cluster, and following both from high cluster symmetry and from equivalence of the configurations as a result of the electron transitions.

**Acknowledgment.** The authors acknowledge the reviewers for their helpful comments.

IC7006974

(47) Black, T. D.; Rubins, R. S.; De, D. K.; Dickinson, R. C.; Baker, W. A., Jr. *J. Chem. Phys*. **1984**, *80*, 4620−4624.